SPEED-RL: Faster Training of Reasoning Models via Online Curriculum Learning

Ruiqi Zhang
Department of Statistics
University of California, Berkeley
rqzhang@berkeley.edu

Daman Arora
Machine Learning Department
Carnegie Mellon University
damana@andrew.cmu.edu

Song Mei
Department of Statistics
University of California, Berkeley
songmei@berkeley.edu

Andrea Zanette
Department of ECE
Carnegie Mellon University
zanette@cmu.edu

Abstract

Training large language models with reinforcement learning (RL) against verifiable rewards significantly enhances their reasoning abilities, yet remains computationally expensive due to inefficient uniform prompt sampling. We introduce SELECTIVE PROMPTING WITH EFFICIENT ESTIMATION OF DIFFICULTY (**SPEED**), an adaptive online RL curriculum that selectively chooses training examples of intermediate difficulty to maximize learning efficiency. Theoretically, we establish that intermediate-difficulty prompts improve the gradient estimator's signal-to-noise ratio, accelerating convergence. Empirically, our efficient implementation leads to 2× to 6× faster training without degrading accuracy, requires no manual tuning, and integrates seamlessly into standard RL algorithms.

1 Introduction

Training large reasoning models (LLMs) commonly employs reinforcement learning (RL) techniques [Sutton et al., 1999] guided by automated verifiers [Ahmadian et al., 2024, Guo et al., 2025]. However, this approach is computationally expensive, often surpassing the costs associated with conventional supervised fine-tuning. The substantial computational overhead constitutes a significant bottleneck for developing bespoke reasoning models for specific downstream tasks. Given the increasing importance of advanced reasoning skills across various domains, it is crucial to devise more compute-efficient strategies to train models with RL without sacrificing performance quality. This paper introduces and investigates data-driven techniques aimed at accelerating RL-based training of reasoning models.

Previous literature has demonstrated state-of-the-art reasoning performance by training LLMs on carefully curated datasets [Muennighoff et al., 2025, Ye et al., 2025, Li et al., 2025]. However, these approaches predominantly depend on extensive human manual effort during data selection, limiting their scalability and practical flexibility. One attractive way to accelerate the training of reasoning models is to use *curriculum learning*, a training methodology that progressively organizes examples from simple to difficult. While curriculum learning has produced impressive results in some machine learning domains, it has yielded mixed or minimal improvements in others [Bengio et al., 2009, Soviany et al., 2022]. On the other hand, the effectiveness of curriculum learning specifically integrated into RL training of LLMs for reasoning tasks remains poorly understood.

In this work, we propose a data-driven **online curriculum learning** strategy that dynamically prioritizes and selects informative training samples during RL training based on real-time estimates

Preprint. Under review.

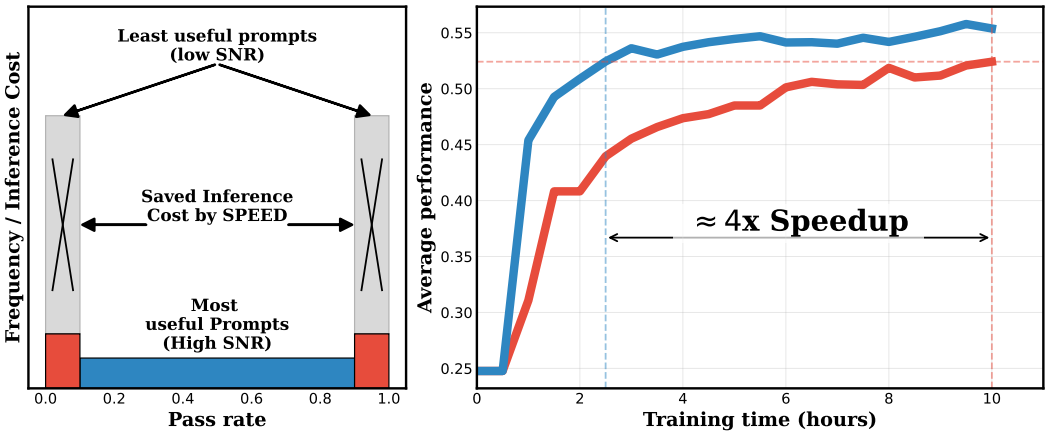

Figure 1: Left: The impact of our proposed algorithm, **SPEED**, on accelerating RL training of LLMs. SPEED reduces inference costs by excluding extremely easy or overly difficult prompts, focusing RL fine-tuning exclusively on moderately challenging prompts that offer the highest signal-to-noise ratio. Right: We report accuracy averaged across five benchmarks and four training configurations, comparing both variants of SPEED against baseline RL algorithms. We conduct experiments using Qwen2.5-Math-7B.

of difficulty. While similar insights have been explored in prior literature [Yang et al., 2024, Guo et al., 2025, Team et al., 2025, Foster and Foerster, 2025] and concurrent works [Bae et al., 2025, Lin et al., 2025, Yu et al., 2025, Xu et al., 2025, Cui et al., 2025], these methods have typically not yet realized the full potential of online curriculum learning—specifically, a substantial reduction in *wall-clock* RL training time for reasoning models. To address this gap, this paper makes two primary contributions—one theoretical and one methodological—each reinforcing the other.

1.1 Theoretical contribution

We rigorously demonstrate that prompts of intermediate difficulty levels provide the strongest learning signal within RL frameworks. Specifically, we establish a novel theoretical connection between the prompt *pass rate*—defined as the probability of a model correctly solving a given question—and the *signal-to-noise ratio (SNR)* of stochastic gradient estimators, which critically influences the performance of stochastic optimization algorithms. Our analysis reveals that the gradient estimator's SNR significantly deteriorates for prompts with pass rates near 0% or 100%, where stochastic gradients become dominated by noise, making additional sampling meaningless. Crucially, our theoretical findings generalize to many widely-used policy gradient algorithms, such as REINFORCE[Sutton et al., 1999], REINFORCE++[Hu, 2025], RLOO[Ahmadian et al., 2024], GRPO[Shao et al., 2024], and PPO[Schulman et al., 2017], and extend to domains beyond reasoning and language models. These insights directly inform our methodological approach.

1.2 Design principle and practical implementation

Guided by our theoretical insights, we introduce an efficient online curriculum learning framework that dynamically selects prompts at optimal difficulty levels for RL training. To achieve a lightweight online curriculum implementation, our procedure leverages the current state of the model itself to estimate the prompt difficulty. An instantiation of this idea is found in Foster and Foerster [2025], where many candidate responses per prompt are generated through full inference to estimate pass rates, and only informative prompts are selected for training (i.e., performing forward and backward passes to update models' weights). However, this vanilla implementation offers limited practical acceleration, as it does not address the heavy cost of inference, which is typically the most computationally demanding phase of RL training that dominates other costs, including gradient computation and parameter updates.

On the contrary, our design reduces inference costs and enhances the quality of training signals for prompts selected during training, enabling more effective updates and faster convergence. In

practice, we implement this by *screening prompts for pass rates prior to performing expensive full inference*, subsequently conducting full inference only on prompts with suitable difficulty levels, directly reducing the computational overhead associated with the most intensive component of RL training. Specifically, we employ a lightweight statistical test to quickly estimate prompt difficulty, combined with an optimized pre-fetching mechanism that reduces inference overhead. Experimental evaluations demonstrate substantial **wall-clock** speedups: our method **accelerates RL training by 2x to 6x** compared to baseline RL algorithms to achieve the same target performance across standard mathematical reasoning benchmarks. Furthermore, our curriculum method requires no manual data preprocessing or specialized auxiliary neural components, integrates seamlessly with prevalent RL algorithms (e.g., GRPO, REINFORCE, RLOO), and is broadly applicable to many tasks with binary-verifiable rewards.

Our code is available at `https://github.com/Zanette-Labs/speed-rl`.

2 Problem Setup

Let π_θ denote a language model parameterized by parameters θ. Given a prompt $x \in \mathcal{X}$, the model produces a response $y = (y^1, y^2, \dots) \in \mathcal{Y}$ auto-regressively. Formally, each token in the response sequence is generated according to the conditional probability:

$$y^{k+1} \sim \pi_\theta(\cdot \mid x, y^{\leq k}), \tag{1}$$

where we use $y^{\leq k}$ to refer to the first k tokens generated by the model. For reasoning-based tasks considered here, the model typically produces responses following a step-by-step "chain-of-thought" reasoning approach [Wei et al., 2022]. A verification function $r(y)$ subsequently evaluates the correctness of the model's response based on the ground-truth answer, e.g.,

$$r(y) = \begin{cases} 1 & \text{if } y \text{ is correct,} \\ 0 & \text{if } y \text{ is incorrect.} \end{cases} \tag{2}$$

Our primary objective is to maximize the **pass rate**, defined as the average accuracy of the model π_θ across a distribution of prompts $\mathcal{D}_\mathcal{X}$. Explicitly, the optimization objective is defined as follows:

$$J(\theta) = \mathbb{E}_{x \sim \mathcal{D}_\mathcal{X}} \mathbb{E}_{y \sim \pi_\theta(\cdot|x)}[r(y)], \tag{3}$$

where $\mathcal{D}_\mathcal{X}$ is a distribution over the prompt set. Taking the gradient of the objective (3) with respect to model parameters θ and employing a baseline (for variance reduction) [Sutton et al., 1999] leads to the well-known policy gradient formulation:

$$\nabla_\theta J(\theta) = \mathbb{E}_{x \sim \mathcal{D}_\mathcal{X}} \mathbb{E}_{y \sim \pi_\theta(\cdot|x)} \left[\mathcal{A}(y) \nabla_\theta \log \pi_\theta(y \mid x) \right], \tag{4}$$

where the advantage function $\mathcal{A}(y)$ is given by:

$$\mathcal{A}(y) = r(y) - \mathbb{E}_{y' \sim \pi_\theta(\cdot|x)}[r(y')]. \tag{5}$$

Here $\mathbb{E}_{y' \sim \pi_\theta(\cdot|x)}[r(y')]$ is the expected pass rate for prompt x. In practice, the policy gradient in equation (4) is estimated through Monte Carlo samples, yielding the classical *REINFORCE* algorithm [Sutton et al., 1999]. Recent works have further modified this base policy gradient formulation to improve its stability, efficiency, and practicality. This has resulted in advanced methods such as REINFORCE++ [Hu, 2025], GRPO [Shao et al., 2024], PPO [Schulman et al., 2017], and RLOO [Ahmadian et al., 2024].

3 What Prompts Lead to Useful Training Signal?

Our work builds on the observation, also noted in prior studies, that many training prompts are either too easy or too hard, thereby offering limited useful learning signals (see e.g., [Foster and Foerster, 2025, Yu et al., 2025, Schaeffer et al., 2025]). Figure 2 concretely illustrates this point: for 1000 prompts randomly selected from the DAPO-17k dataset, we evaluated Qwen 2.5-Math-1.5B and Qwen 2.5-Math-7B by sampling 50 completions per prompt. Even with this extensive sampling, approximately 34% and 25.8% of prompts, respectively, have a pass rate exactly equal to zero, that is, none of the model's attempts to solve the question succeeded. Intuitively, prompts that are either too difficult or too simple provide limited training signals because models gain minimal information from consistently incorrect responses (too difficult) or consistently correct responses (too easy), reducing the effectiveness of gradient updates. We formalize and substantiate this intuition rigorously in this section using information-theoretic tools.

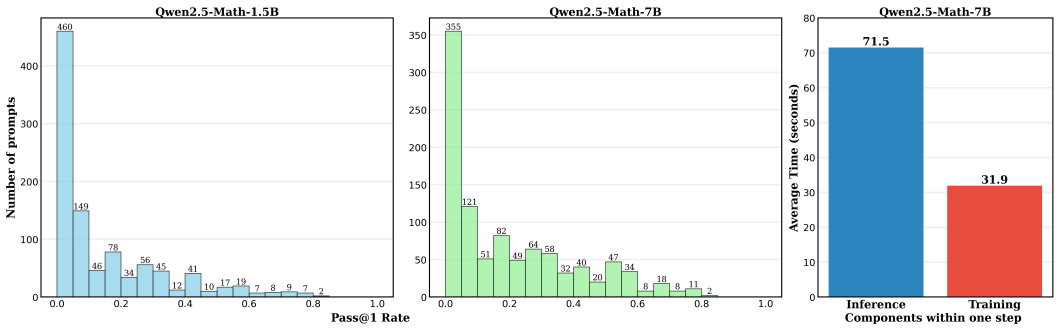

Figure 2: Left and middle: Pass rate distribution of 1000 samples in DAPO-17k evaluated by Qwen2.5-Math-1.5B (left) and Qwen2.5-Math-7B (middle). To evaluate the pass rates, we sample 50 responses per prompt. Right: Average per-step inference and training times while running RLOO on the Qwen2.5-Math-7B model.

3.1 The Signal-to-Noise ratio

When the pass rate for prompt x is either 0% or 100%, the advantage function—and hence the policy gradient—is exactly zero:

$$\nabla_\theta J_x(\theta) = \mathbb{E}_{y\sim\pi_\theta(\cdot|x)}\big[\underbrace{\mathcal{A}(y)}_{=0}\nabla_\theta \log \pi_\theta(y \mid x)\big] = 0, \qquad \text{if the pass rate is } 0\% \text{ or } 100\%. \tag{6}$$

Thus, these prompts can be removed without affecting the gradient. This observation leads us to develop a more solid theory, which uses information-theoretic tools to measure the utility of a prompt.

A natural measure quantifying the informativeness of a prompt is the *Signal-to-Noise Ratio (SNR)* of the policy gradient estimate. Typically, one estimates the policy gradient in (6) via Monte Carlo samples:

$$\widehat{\nabla_\theta J_x}(\theta) = \frac{1}{N}\sum_{i=1}^{N} \widehat{\mathcal{A}}(y_i)\cdot\nabla_\theta \log \pi_\theta(y_i \mid x), \quad \text{where} \quad y_1, ..., y_N \overset{i.i.d.}{\sim} \pi_\theta(\cdot \mid x). \tag{7}$$

Here, $\widehat{\mathcal{A}}(y_i)$ is the advantage estimate for response y_i. For example, in our experiments, we adopt the RLOO estimator from Ahmadian et al. [2024]:

$$\widehat{\mathcal{A}}(y_i) := r(y_i) - \frac{1}{N-1}\sum_{j\neq i} r(y_j). \tag{8}$$

With this definition, the empirical policy-gradient in (7) is an unbiased estimator of the true gradient. The SNR is then defined as the ratio between the squared norm of the gradient estimator and its variance:

$$\mathrm{SNR}(\theta) := \frac{\|\mathbb{E}\widehat{\nabla_\theta J_x}(\theta)\|^2}{\mathbb{E}\|\widehat{\nabla_\theta J_x}(\theta) - \mathbb{E}\widehat{\nabla_\theta J_x}(\theta)\|^2}. \tag{9}$$

Here, the SNR is a function of the model parameter θ and prompt x. It quantifies the amount of information carried by a stochastic gradient, and it governs the expected improvement of methods based on stochastic gradients—such as RLOO, PPO, REINFORCE, etc. A simple connection between the SNR and the expected improvements is revealed in the following fact.

Fact 1 *Consider the one-step stochastic gradient update $\theta^+ = \theta + \widehat{\nabla_\theta J_x}(\theta)$, where the empirical policy gradient is unbiased. Assume $J_x(\theta)$ defined in* (4) *is 1-smooth. Then, one has*

$$\mathbb{E}[J_x(\theta^+)] - J_x(\theta) \geq \frac{1}{2}\|\nabla_\theta J_x(\theta)\|^2\left(1 - \frac{1}{\mathrm{SNR}(\theta)}\right), \tag{10}$$

where SNR is defined as (9).

This can be viewed as a natural consequence of the standard analysis of SGD on smooth functions [Duchi, 2018, Bernstein et al., 2018]. We include the proof in Appendix A for completeness. Thus, if the SNR approaches zero, the variance completely overwhelms the signal, and negligible improvement is expected from a single update step. Conversely, as the SNR increases toward infinity, we recover the fast convergence behavior characteristic of deterministic gradient methods.

3.2 A fundamental connections between the SNR and the pass rate

A straightforward technique to increase the SNR is to simply increase the number of sampled rollouts. Doing so reduces the variance of the gradient estimator—the denominator of the SNR. However, this straightforward approach involves additional compute.

In this work, instead, we select the most informative prompts to enhance the SNR during training, thus framing curriculum learning as a variance reduction technique. More precisely, we establish an explicit link between the gradient estimator's SNR and the prompt pass rate $\mathcal{P} = \mathbb{E}_{y\sim\pi_\theta(\cdot|x)}[\mathbb{I}(r(y) = 1)]$ for a given prompt x. Note that the pass rate depends on both the prompt and the generative model. We obtain the following fundamental result, whose proof is deferred to Appendix A.

Theorem 3.1 (Fundamental Connection between SNR and Pass Rate) *Fix a prompt x. Let $\mathcal{P}_x(\theta)$ denote the pass rate of prompt x under the current policy $(\pi_\theta(\cdot|x))$: $\mathcal{P}_x(\theta) = \mathbb{E}_{y\sim\pi_\theta(\cdot|x)}[\mathbb{I}(r(y) = 1)]$. The SNR of the stochastic gradient estimator (defined in (9)) for $N \geq 3$ and $p < 1/4$ or $p > 3/4$ satisfies the bound*

$$\mathrm{SNR} \leq 4N \cdot \mathcal{P}_x(\theta)(1 - \mathcal{P}_x(\theta)). \tag{11}$$

Moreover, for fixed N, we have

$$\lim_{\mathcal{P}_x(\theta)\to 1} \mathrm{SNR} = \lim_{\mathcal{P}_x(\theta)\to 0} \mathrm{SNR} = 0.$$

This result is significant because it explicitly quantifies how much informative signal (relative to noise) a single training step provides as a direct function of pass rate. Crucially, Theorem 3.1 confirms an important intuition: prompts with very low ($\mathcal{P} \approx 0\%$) or very high ($\mathcal{P} \approx 100\%$) pass rates both yield vanishing SNR. Such prompts provide negligible useful training signal while potentially introducing detrimental variance in parameter updates. Therefore, the fundamental insight established by theorem 3.1 is the following.

Optimal curricula must explicitly prioritize intermediate-difficulty prompts in order to maximize learning signal and effectiveness.

4 SPEED-RL

In this section, we introduce SELECTIVE PROMPTING WITH EFFICIENT ESTIMATION OF DIFFICULTY (SPEED), an online curriculum learning method designed to feed training prompts at the appropriate level of difficulty, thus maximizing learning efficiency. We first introduce the algorithm design, and then provide a theoretical justification for our proposed method in Section 4.2. Finally, we provide several efficient implementation schemes in Section 4.3.

4.1 Algorithm design

Since the model proficiency evolves throughout training, prompt difficulties must be continuously reassessed, motivating an *adaptive, on-the-fly* curriculum design. However, reliably identifying informative prompts in a general and computationally efficient manner is challenging. Naively estimating prompt difficulties by generating multiple responses per prompt (as studied recently in Foster and Foerster [2025]) and computing pass rates quickly becomes computationally prohibitive since inference typically dominates RL training time. As demonstrated in Figure 2, inference time for methods like RLOO often exceeds the actual gradient update time by a factor of two, even for moderately lengthy responses. Therefore, achieving real wall-clock time speedup necessitates efficiently screening prompts *before* full inference.

Typically, RL methods generate N rollouts per prompt (commonly $N = 16$ to 64 [Liu et al., 2024, Guo et al., 2025, Yu et al., 2025]). To improve efficiency, we propose a two-phase inference approach:

1. **Screening Phase**: Initially, we generate a small number ($N_{\mathsf{init}} \approx 4$–$8$) of responses per prompt. Although insufficient for reliable gradient estimation, those generations efficiently identify prompts whose estimated pass rates fall distinctly away from trivial extremes (near-0% or near-100%). Such prompts are termed **qualified prompts**.
2. **Continuation Phase**: For qualified prompts identified in the screening phase, we then generate the remaining N_{cont} responses, completing the total of N rollouts per prompt. This *ensures computational resources are allocated primarily to prompts offering high SNR.*

Our two-phase inference scheme integrates seamlessly with widely-used RL algorithms, including GRPO, PPO, RLOO, and REINFORCE. The procedure is detailed in algorithm 1.

Algorithm 1 Selective Prompting with Efficient Estimation of Difficulty (SPEED)

Input: The screening size N_{init} and the continuation size N_{cont}.
for step $t = 1, 2, \ldots$ **do**
  $\mathcal{D}_{\mathsf{accepted}} \leftarrow \emptyset$
  while $|\mathcal{D}_{\mathsf{accepted}}| <$ training batch size **do**
    Sample prompt $x \in \mathcal{X}$.
    Generate N_{init} responses from current model
    $\textsc{PassRate}(x) \leftarrow \frac{1}{N_{\mathsf{init}}} \sum_{i=1}^{N_{\mathsf{init}}} \mathbb{I}(\text{response}_i \text{ is correct})$
    if $0 < \textsc{PassRate}(x) < 1$ **then**
      $\mathcal{D}_{\mathsf{accepted}} \leftarrow \mathcal{D}_{\mathsf{accepted}} \cup \{x\}$
    end if
  end while
  for each prompt $x \in \mathcal{D}_{\mathsf{accepted}}$ **do**
    Generate additional N_{cont} responses
  end for
  Perform one RL update step using all $N_{\mathsf{init}} + N_{\mathsf{cont}}$ responses for $x \in \mathcal{D}_{\mathsf{accepted}}$
end for

4.2 Theoretical justifications

Objective function. To make sense of our algorithm design, in this section, we show that SPEED preserves the original learning goal by characterizing the objective it implicitly optimizes when combined with RLOO. The theorem makes use of a monotonically increasing function $\Phi(\cdot) : [0, 1] \to [0, 1]$, detailed in Appendix B, which is determined solely by $(N_{\mathsf{init}}, N_{\mathsf{cont}})$.

Theorem 4.1 *Run SPEED (Algorithm 1) with screening size $N_{\mathsf{init}} \geq 1$, continuation size $N_{\mathsf{cont}} \geq 1$, and the RLOO advantage estimator in* (8)*. This implicitly optimizes the following objective*

$$\overline{J}(\theta) = \mathbb{E}_{x \sim \mathcal{D}_{\mathcal{X}}} \left[\Phi(\mathbb{E}_{y \sim \pi_\theta(\cdot|x)}[r(y)]) \right]. \tag{12}$$

Moreover, $\overline{J}(\theta)$ is maximized when

$$\mathbb{E}_{y \sim \pi_\theta(\cdot|x)}[r(y)] = 1 \quad \textit{for every prompt} \quad x \in \mathcal{X}.$$

The theorem confirms that SPEED merely reweights prompts via the monotone map Φ. It does not change the set of optimal policies. In other words, *SPEED accelerates training without sacrificing the ultimate objective of attaining perfect pass rates on every prompt*. The complete form of $\Phi(\cdot)$ and the proof are deferred to Appendix B.

4.3 Efficient implementation

Implementing two-phase inference with a single call. The two-phase inference approach aims to maximize completions with high SNR while minimizing computations on prompts with low SNR. A naive implementation would separately invoke the inference engine (e.g., vLLM [Kwon et al., 2023]) twice: once for each inference phase. However, performing two separate calls introduces unnecessary computational overhead.

To address this, we introduce a pre-fetching mechanism that implements both the *screening* and *continuation* phases within a single inference call, significantly enhancing computational efficiency.

Specifically, we combine the *continuation phase* of the current batch—consisting of qualified prompts identified earlier—with the *screening phase* for the next batch of prompts into one unified inference request. This batching strategy leverages GPU efficiency due to improved parallelism and reduced overhead from multiple inference calls.

Sampling buffer. Typically, the training batch size is a fixed hyper-parameter, chosen to balance computational efficiency and training stability. However, this static setting conflicts with our proposed curriculum learning approach, as the number of qualified prompts dynamically fluctuates based on real-time pass-rate estimations, potentially causing significant deviations from the target batch size.

To maintain a consistent training batch size, we introduce a *sampling buffer*, which temporarily stores qualified prompts that exceed the current batch-size limit, deferring full inference to subsequent training steps. This mechanism prevents redundant inference computations and avoids inefficient multiple inference calls.

While buffering introduces a modest increase in off-policy data, experimental evaluations clearly demonstrate that this strategy significantly enhances computational efficiency without negatively impacting performance. A detailed description of the complete algorithm, combining the sampling buffer and pre-fetching mechanisms, is provided in Algorithm 2.

5 Experiments

In this section, we evaluate the performance of **SPEED**. We first describe our experimental setup, including the models, datasets, baseline methods, and evaluation metrics. We then present our primary results and discussions in Section 5.2.

5.1 Training setup

Our experiments use Qwen2.5-Math-1.5B and Qwen2.5-Math-7B models [Yang et al., 2024]. We integrate SPEED with two rule-based RL methods: RLOO [Ahmadian et al., 2024] and DAPO [Yu et al., 2025]. DAPO serves as an important baseline for curriculum learning as it filters all prompts with 0% or 100% pass rates after generating all responses. While our evaluation focuses on these two algorithms, our approach is broadly applicable to any rule-based RL method.

We train the models using three large scale datasets: NuminaMath [Li et al., 2024], DAPO-17k [Yu et al., 2025], and DeepScaleR [Luo et al., 2025]. NuminaMath originally contains 860k prompts, ranging from simpler GSM8k [Cobbe et al., 2021] and MATH [Hendrycks et al., 2021] questions to challenging competition-level problems. We filter out proof-based questions and keep only problems with integer-valued solutions, which leaves us with 220k prompts. The DAPO-17k dataset consists of 17k integer-answer prompts, of which we reserve 1k as a held-out test set and use the remaining prompts for training. DeepScaleR contains approximately 400k training examples derived from past AIME (up to 2023) and AMC (prior to 2023) competitions. Besides the held-out test set in DAPO-17k, we evaluate the models' performance on four additional standard mathematical reasoning datasets: MATH500 [Lightman et al., 2023], AIME2024 [AIM, 2024], AIME2025 [AIM, 2024], and AMC2023 [AMC, 2023].

We measure SPEED's efficiency improvements by comparing the relative wall-clock time needed to reach specific accuracy targets. When calculating the training time, we include every stage in the RL training except the time for validation and saving checkpoints. To ensure consistency, all experiments use a single node equipped with four NVIDIA GH200 GPUs (with 96GB of GPU memory and 120GB CPU memory each). Our implementation relies on the VeRL framework [Sheng et al., 2024]. Unless otherwise specified, the training batch size (number of prompts) is set to 16, and the generation batch size is 64 for SPEED variants. For vanilla DAPO and SPEED-DAPO, we set $\varepsilon_{\mathsf{low}} = 0.2, \varepsilon_{\mathsf{high}} = 0.28$. In every experiment, we apply a learning rate of 10^{-6} with a warmup period of 10 steps and a weight decay of 0.1. Baselines generate $N = 24$ responses per prompt, and SPEED-RL variants use a combined $N_{\mathsf{init}} + N_{\mathsf{cont}} = 24$ generations.

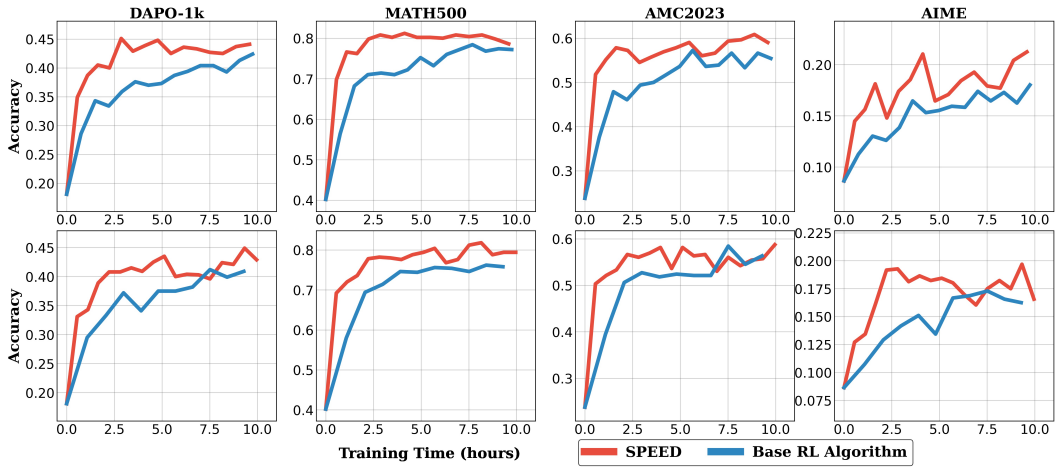

Figure 3: Validation accuracy on various mathematical reasoning benchmarks for SPEED-variants of RL algorithms, and base RL algorithms. Top: RLOO versus SPEED-RLOO; bottom: DAPO versus SPEED-DAPO. The initial model used is Qwen2.5-Math-7B, trained on the DeepScaleR dataset.

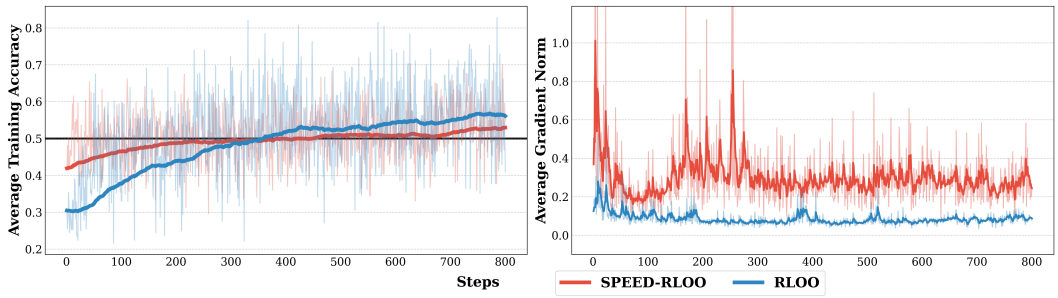

Figure 4: Average training accuracy (left) and gradient norm (right) comparison between RLOO and SPEED-RLOO during training of Qwen2.5-Math-7B. For the SPEED variants, the reported accuracies on the training set are calculated exclusively using the qualified prompts that are selected in the actual training process, showing that the SPEED variant keeps feeding data at a near optimal level of difficulty even if the model's capabilities increase.

5.2 Results

Figure 3 and Table 1 illustrate that SPEED significantly enhances training efficiency when fine-tuning base models on widely adopted datasets such as DAPO-17k [Yu et al., 2025], NuminaMath [Li et al., 2024], and DeepScaleR [Luo et al., 2025]. Integrated with rule-based RL algorithms RLOO and DAPO, SPEED achieves target validation accuracies 2–6 times faster compared with baseline RL algorithms across nearly all benchmarks and experimental runs. For instance, on DAPO-1k, Qwen2.5-Math-7B reaches a validation accuracy of 0.45 in 7.6 hours with SPEED-RLOO, whereas vanilla RLOO requires approximately 3.4 times longer. Although specific speedup values vary by dataset and target accuracy, our results consistently demonstrate substantial efficiency improvements across multiple setups.

Informativeness of gradient updates To understand why SPEED improves efficiency, we examine the informativeness of gradients produced during training. As depicted in Figure 4, SPEED-RLOO consistently maintains training accuracies much closer to 0.5 compared to vanilla RLOO, particularly in early training stages. According to our theoretical analysis (Theorem 3.1), prompts with pass rates close to 0.5 yield higher SNR, which enhances training efficiency. Additionally, gradient norms from SPEED-RLOO are substantially larger than those from baseline methods.

Effect of N_{init}. The initial inference stage generation count (N_{init}) is effectively the only additional hyperparameter introduced by our method. A larger N_{init} increases the likelihood of selecting prompts

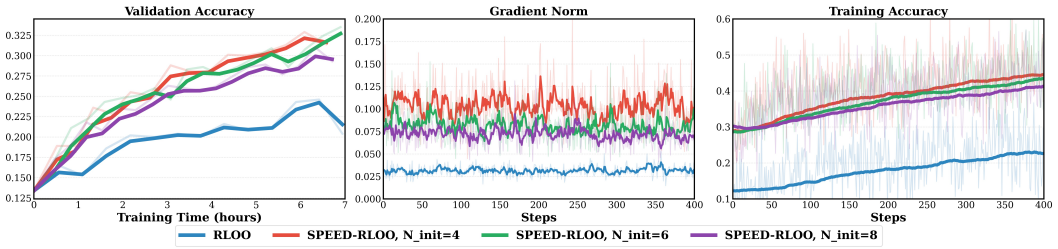

Figure 5: The validation accuracy on DAPO-1k (left), the average gradient norm (middle), and the average training accuracy (right) of RLOO and SPEED-RLOO with different N_{init}. Notice that the training accuracy (right) refers to the prompts screened for optimal pass rate. We train Qwen2.5-Math-1.5B on the training split of DAPO-17k.

Table 1: Wall-clock training hours needed for each model to reach a target accuracy on its respective benchmark. For the Qwen-Math-1.5B model, the targets are 0.30 on DAPO-1k, 0.70 on MATH500, 0.4 on AMC2023, and 0.10 on AIME. For the larger Qwen2.5-Math-7B model, the thresholds increase to 0.45, 0.80, 0.55, and 0.18 for the same datasets, respectively. Validation time and checkpoint-saving overhead are excluded. Values in parentheses give the corresponding wall-clock speed-ups. † means the performance has not reached the threshold during the entire training process. The average speedups reported across benchmarks and training configurations are computed as the simple arithmetic mean of individual speedup values.

Model Size	Training Data	Algorithm	DAPO-1k	MATH500	AMC2023	AIME	Average
Math-1.5B	NuminaMath	RLOO	25.9	13.6	4.7	13.6	**2.8 x**
		SPEED-RLOO	7.6 (**3.4 x**)	3.3 (**4.1 x**)	2.8 (**1.7 x**)	6.4 (**2.1 x**)	
		DAPO	†	18.0	10.0	16.7	**3.0 x**
		SPEED-DAPO	11.6 (†)	3.9 (**4.6 x**)	3.4 (**2.9 x**)	10.4 (**1.6 x**)	
	DAPO-17k	RLOO	†	13.8	8.0	12.8	**3.1 x**
		SPEED-RLOO	4.4 (†)	4.8 (**2.9 x**)	2.2 (**3.6 x**)	4.8 (**2.7 x**)	
Math-7B	DAPO-17k	RLOO	13.5	12.7	4.3	7.8	**3.0 x**
		SPEED-RLOO	3.6 (**3.8 x**)	4.3 (**3.0 x**)	1.8 (**2.4 x**)	3.0 (**2.6 x**)	
		DAPO	12.1	21.8	7.6	7.6	**3.0 x**
		SPEED-DAPO	5.0 (**2.4 x**)	6.2 (**3.5 x**)	2.2 (**3.5 x**)	2.8 (**2.7 x**)	
	DeepScaleR	RLOO	12.6	11.1	5.6	9.7	**4.8 x**
		SPEED-RLOO	2.9 (**4.3 x**)	2.9 (**3.8 x**)	1.1 (**5.1 x**)	1.6 (**6.1 x**)	
		DAPO	17.1	16.2	7.5	11.1	**3.1 x**
		SPEED-DAPO	15.1 (**1.1 x**)	5.7 (**2.8 x**)	2.2 (**3.4 x**)	2.2 (**5.0 x**)	
Average Speedup			**3.0 x**	**3.5 x**	**3.2 x**	**3.3 x**	**3.3 x**

with more extreme pass rates, potentially reducing gradient informativeness. Figure 5 compares setups with $N_{\text{init}} = 4, 6, 8$ under identical conditions. Results show that larger N_{init} values lead to smaller average gradient norms and push training accuracies away from 0.5. This aligns with our theoretical insights that the prompts with pass rates near 0.5 can provide stronger learning signals. As a result, increasing N_{init} tends to slow down the performance rise and reduce the efficiency improvements compared to baselines.

6 Additional Related Works

Large reasoning models and reinforcement learning. Large language models (LLMs) have achieved remarkable performance on mathematical reasoning and code generation [Achiam et al., 2023, Yang et al., 2024, Jaech et al., 2024, Hurst et al., 2024, Lambert et al., 2024, Guo et al., 2025, Team et al., 2025]. Fine-tuning these pretrained models often relies on reinforcement learning (RL) methods such as Proximal Policy Optimization (PPO) [Schulman et al., 2017, Hu et al., 2025]. However, PPO updates can be computationally expensive and prone to reward hacking, limiting rapid iteration and deployment. To address these issues, several rule-based RL variants have been proposed. DeepSeek, for example, introduces Group Relative Policy Optimization (GRPO) [Shao

et al., 2024, Guo et al., 2025]. Other extensions—such as REMAX [Li et al., 2023], RLOO [Ahmadian et al., 2024], and REINFORCE++ [Hu, 2025, Xie et al., 2025]—further demonstrate the benefits of rule-based RL.

Difficulty-based curriculum learning. Training large reasoning models is often computationally expensive. *Curriculum learning* arranges training examples by increasing difficulty to guide model learning from moderately difficult examples [Bengio et al., 2009]. Several open-source LLMs (e.g., Qwen2.5 [Yang et al., 2024], Kimi-1.5 [Team et al., 2025]) mention curricula without publishing details. Some *static* methods sort data offline—using pass-rate estimates [Wen et al., 2025], human difficulty labels [Lee et al., 2023], or software metrics for coding tasks [Naïr et al., 2024]—and then apply sequential supervised or RL fine-tuning. Recently, [Shi et al., 2025] estimates the question difficulty offline via the pass rates or from more capable models, and adaptively updates the target difficulty to select proper data in the training stage. In contrast, our method estimates prompt difficulty on the fly, yielding more accurate and timely example selection. Recent work on *online filtering* adapts the curricula to the model's current performance. DAPO [Yu et al., 2025] dynamically samples prompts and discards those with uniformly correct or incorrect responses. Bae et al. [2025], Lin et al. [2025], Meng et al. [2025] further restrict training to prompts with moderate pass rates. [Foster and Foerster, 2025] select the prompts with maximal reward variance. [Xu et al., 2025] adopts a similar idea and further decouples the inference and training phases to boost the efficiency. [Cui et al., 2025] uses a separately trained process reward model to gauge difficulty. Similarly, [Tajwar et al., 2025] employs an online curriculum learning approach to select appropriate decision-making tasks for model training. They estimate the question difficulty via the pass rate after all responses are generated. Unlike these methods, we use a lightweight generation step to infer difficulty, reducing compute and boosting the inference efficiency.

More methods for efficient reasoning. Beyond curriculum learning, researchers have explored data selection and inference optimizations for reasoning models. Curating high-quality chain-of-thought data can boost training efficiency [Muennighoff et al., 2025, Ye et al., 2025, Li et al., 2025], and token-level filtering can further reduce cost [Lin et al., 2024b]. Another class of methods is based on early stopping or rejection sampling, such as RAFT [Dong et al., 2023] and speculative rejection [Sun et al., 2024]. Our method effectively combines early stopping with difficulty filtering.

Other efficient-reasoning approaches compresses chain-of-thoughts via prompt engineering [Han et al., 2024, Nayab et al., 2024], conditional training [Deng et al., 2024, Kang et al., 2025] or RL [Arora and Zanette, 2025, Fatemi et al., 2025]. Additionally, efficient serving systems like vLLM [Kwon et al., 2023], speculative decoding [Leviathan et al., 2023, Liu et al., 2023], weight pruning [Liu et al., 2018], and quantization [Lin et al., 2024a] further cut runtime and memory requirements. These methods are orthogonal to our proposed algorithm and can be seamlessly combined with our method.

7 Conclusion and Future Directions

In this paper, we introduced SPEED, a data-driven approach designed to accelerate RL-based training of large reasoning models through online curriculum learning. By adaptively prioritizing prompts of intermediate difficulty—estimated efficiently via lightweight statistical testing and optimized pre-fetching—SPEED effectively selects the most informative prompts in real-time, substantially improving gradient quality and training efficiency. Our theoretical analysis further reinforced that prompts at moderate difficulty levels optimize the upper bound of the Signal-to-Noise Ratio (SNR), clarifying why such prompts yield maximal learning signals. Empirical evaluations demonstrated notable reductions in training time, achieving two- to six-fold wall-clock speedups across diverse reasoning benchmarks, highlighting SPEED's computational efficiency. Future research opportunities include:

- Exploring curriculum-based methods to enhance peak performance when training over multiple epochs, complementing SPEED's existing efficiency advantages.
- Investigating alternative adaptive selection criteria to estimate the pass rate, such as reward models.
- Integrating reward evaluation directly into efficient inference frameworks (e.g., vLLM) to enable immediate prompt filtering, further reducing computational costs and expanding SPEED's practical applicability.

Acknowledgements

This work has greatly benefited from the use of Delta's advanced computing and data resource supported by the National Science Foundation (OAC 2005572) and the State of Illinois. Overall, this project used ACCESS grants CIS250428 for its compute resources.

References

American mathematics competitions (amc 10/12), 2023, February 2023. URL `https://artofproblemsolving.com/wiki/index.php/AMC_12_Problems_and_Solutions`. Problems and solutions.

American invitational mathematics examination (aime) i and ii, 2024, February 2024. Problems and solutions.

Josh Achiam, Steven Adler, Sandhini Agarwal, Lama Ahmad, Ilge Akkaya, Florencia Leoni Aleman, Diogo Almeida, Janko Altenschmidt, Sam Altman, Shyamal Anadkat, et al. Gpt-4 technical report. *arXiv preprint arXiv:2303.08774*, 2023.

Arash Ahmadian, Chris Cremer, Matthias Gallé, Marzieh Fadaee, Julia Kreutzer, Olivier Pietquin, Ahmet Üstün, and Sara Hooker. Back to basics: Revisiting reinforce style optimization for learning from human feedback in llms. *arXiv preprint arXiv:2402.14740*, 2024.

Daman Arora and Andrea Zanette. Training language models to reason efficiently. *arXiv preprint arXiv:2502.04463*, 2025.

Sanghwan Bae, Jiwoo Hong, Min Young Lee, Hanbyul Kim, JeongYeon Nam, and Donghyun Kwak. Online difficulty filtering for reasoning oriented reinforcement learning. *arXiv preprint arXiv:2504.03380*, 2025.

Yoshua Bengio, Jérôme Louradour, Ronan Collobert, and Jason Weston. Curriculum learning. In *Proceedings of the 26th annual international conference on machine learning*, pages 41–48, 2009.

Jeremy Bernstein, Yu-Xiang Wang, Kamyar Azizzadenesheli, and Animashree Anandkumar. signsgd: Compressed optimisation for non-convex problems. In *International Conference on Machine Learning*, pages 560–569. PMLR, 2018.

Karl Cobbe, Vineet Kosaraju, Mohammad Bavarian, Mark Chen, Heewoo Jun, Lukasz Kaiser, Matthias Plappert, Jerry Tworek, Jacob Hilton, Reiichiro Nakano, et al. Training verifiers to solve math word problems. *arXiv preprint arXiv:2110.14168*, 2021.

Ganqu Cui, Lifan Yuan, Zefan Wang, Hanbin Wang, Wendi Li, Bingxiang He, Yuchen Fan, Tianyu Yu, Qixin Xu, Weize Chen, et al. Process reinforcement through implicit rewards. *arXiv preprint arXiv:2502.01456*, 2025.

Yuntian Deng, Yejin Choi, and Stuart Shieber. From explicit cot to implicit cot: Learning to internalize cot step by step. *arXiv preprint arXiv:2405.14838*, 2024.

Hanze Dong, Wei Xiong, Deepanshu Goyal, Yihan Zhang, Winnie Chow, Rui Pan, Shizhe Diao, Jipeng Zhang, Kashun Shum, and Tong Zhang. Raft: Reward ranked finetuning for generative foundation model alignment. *arXiv preprint arXiv:2304.06767*, 2023.

John C Duchi. Introductory lectures on stochastic optimization. *The mathematics of data*, 25:99–186, 2018.

Mehdi Fatemi, Banafsheh Rafiee, Mingjie Tang, and Kartik Talamadupula. Concise reasoning via reinforcement learning. *arXiv preprint arXiv:2504.05185*, 2025.

Thomas Foster and Jakob Foerster. Learning to reason at the frontier of learnability. *arXiv preprint arXiv:2502.12272*, 2025.

Daya Guo, Dejian Yang, Haowei Zhang, Junxiao Song, Ruoyu Zhang, Runxin Xu, Qihao Zhu, Shirong Ma, Peiyi Wang, Xiao Bi, et al. Deepseek-r1: Incentivizing reasoning capability in llms via reinforcement learning. *arXiv preprint arXiv:2501.12948*, 2025.

Tingxu Han, Zhenting Wang, Chunrong Fang, Shiyu Zhao, Shiqing Ma, and Zhenyu Chen. Token-budget-aware llm reasoning. *arXiv preprint arXiv:2412.18547*, 2024.

Dan Hendrycks, Collin Burns, Saurav Kadavath, Akul Arora, Steven Basart, Eric Tang, Dawn Song, and Jacob Steinhardt. Measuring mathematical problem solving with the math dataset. *arXiv preprint arXiv:2103.03874*, 2021.

Jian Hu. Reinforce++: A simple and efficient approach for aligning large language models. *arXiv preprint arXiv:2501.03262*, 2025.

Jingcheng Hu, Yinmin Zhang, Qi Han, Daxin Jiang, Xiangyu Zhang, and Heung-Yeung Shum. Open-reasoner-zero: An open source approach to scaling up reinforcement learning on the base model. *arXiv preprint arXiv:2503.24290*, 2025.

Aaron Hurst, Adam Lerer, Adam P Goucher, Adam Perelman, Aditya Ramesh, Aidan Clark, AJ Ostrow, Akila Welihinda, Alan Hayes, Alec Radford, et al. Gpt-4o system card. *arXiv preprint arXiv:2410.21276*, 2024.

Aaron Jaech, Adam Kalai, Adam Lerer, Adam Richardson, Ahmed El-Kishky, Aiden Low, Alec Helyar, Aleksander Madry, Alex Beutel, Alex Carney, et al. Openai o1 system card. *arXiv preprint arXiv:2412.16720*, 2024.

Yu Kang, Xianghui Sun, Liangyu Chen, and Wei Zou. C3ot: Generating shorter chain-of-thought without compromising effectiveness. In *Proceedings of the AAAI Conference on Artificial Intelligence*, volume 39, pages 24312–24320, 2025.

Woosuk Kwon, Zhuohan Li, Siyuan Zhuang, Ying Sheng, Lianmin Zheng, Cody Hao Yu, Joseph Gonzalez, Hao Zhang, and Ion Stoica. Efficient memory management for large language model serving with pagedattention. In *Proceedings of the 29th Symposium on Operating Systems Principles*, pages 611–626, 2023.

Nathan Lambert, Jacob Morrison, Valentina Pyatkin, Shengyi Huang, Hamish Ivison, Faeze Brahman, Lester James V Miranda, Alisa Liu, Nouha Dziri, Shane Lyu, et al. T\" ulu 3: Pushing frontiers in open language model post-training. *arXiv preprint arXiv:2411.15124*, 2024.

Bruce W Lee, Hyunsoo Cho, and Kang Min Yoo. Instruction tuning with human curriculum. *arXiv preprint arXiv:2310.09518*, 2023.

Yaniv Leviathan, Matan Kalman, and Yossi Matias. Fast inference from transformers via speculative decoding. In *International Conference on Machine Learning*, pages 19274–19286. PMLR, 2023.

Jia Li, Edward Beeching, Lewis Tunstall, Ben Lipkin, Roman Soletskyi, Shengyi Huang, Kashif Rasul, Longhui Yu, Albert Q Jiang, Ziju Shen, et al. Numinamath: The largest public dataset in ai4maths with 860k pairs of competition math problems and solutions. *Hugging Face repository*, 13:9, 2024.

Xuefeng Li, Haoyang Zou, and Pengfei Liu. Limr: Less is more for rl scaling. *arXiv preprint arXiv:2502.11886*, 2025.

Ziniu Li, Tian Xu, Yushun Zhang, Zhihang Lin, Yang Yu, Ruoyu Sun, and Zhi-Quan Luo. Remax: A simple, effective, and efficient reinforcement learning method for aligning large language models. *arXiv preprint arXiv:2310.10505*, 2023.

Hunter Lightman, Vineet Kosaraju, Yuri Burda, Harrison Edwards, Bowen Baker, Teddy Lee, Jan Leike, John Schulman, Ilya Sutskever, and Karl Cobbe. Let's verify step by step. In *The Twelfth International Conference on Learning Representations*, 2023.

Ji Lin, Jiaming Tang, Haotian Tang, Shang Yang, Wei-Ming Chen, Wei-Chen Wang, Guangxuan Xiao, Xingyu Dang, Chuang Gan, and Song Han. Awq: Activation-aware weight quantization for on-device llm compression and acceleration. *Proceedings of Machine Learning and Systems*, 6: 87–100, 2024a.

Zhenghao Lin, Zhibin Gou, Yeyun Gong, Xiao Liu, Yelong Shen, Ruochen Xu, Chen Lin, Yujiu Yang, Jian Jiao, Nan Duan, et al. Rho-1: Not all tokens are what you need. *arXiv preprint arXiv:2404.07965*, 2024b.

Zhihang Lin, Mingbao Lin, Yuan Xie, and Rongrong Ji. Cppo: Accelerating the training of group relative policy optimization-based reasoning models. *arXiv preprint arXiv:2503.22342*, 2025.

Aixin Liu, Bei Feng, Bing Xue, Bingxuan Wang, Bochao Wu, Chengda Lu, Chenggang Zhao, Chengqi Deng, Chenyu Zhang, Chong Ruan, et al. Deepseek-v3 technical report. *arXiv preprint arXiv:2412.19437*, 2024.

Xiaoxuan Liu, Lanxiang Hu, Peter Bailis, Alvin Cheung, Zhijie Deng, Ion Stoica, and Hao Zhang. Online speculative decoding. *arXiv preprint arXiv:2310.07177*, 2023.

Zhuang Liu, Mingjie Sun, Tinghui Zhou, Gao Huang, and Trevor Darrell. Rethinking the value of network pruning. *arXiv preprint arXiv:1810.05270*, 2018.

Michael Luo, Sijun Tan, Justin Wong, Xiaoxiang Shi, William Tang, Manan Roongta, Colin Cai, Jeffrey Luo, Tianjun Zhang, Erran Li, Raluca Ada Popa, and Ion Stoica. Deepscaler: Surpassing o1-preview with a 1.5b model by scaling rl, 2025.

Fanqing Meng, Lingxiao Du, Zongkai Liu, Zhixiang Zhou, Quanfeng Lu, Daocheng Fu, Tiancheng Han, Botian Shi, Wenhai Wang, Junjun He, et al. Mm-eureka: Exploring the frontiers of multimodal reasoning with rule-based reinforcement learning. *arXiv preprint arXiv:2503.07365*, 2025.

Niklas Muennighoff, Zitong Yang, Weijia Shi, Xiang Lisa Li, Li Fei-Fei, Hannaneh Hajishirzi, Luke Zettlemoyer, Percy Liang, Emmanuel Candès, and Tatsunori Hashimoto. s1: Simple test-time scaling, 2025. URL `https://arxiv.org/abs/2501.19393`.

Marwa Naïr, Kamel Yamani, Lynda Said Lhadj, and Riyadh Baghdadi. Curriculum learning for small code language models. *arXiv preprint arXiv:2407.10194*, 2024.

Sania Nayab, Giulio Rossolini, Marco Simoni, Andrea Saracino, Giorgio Buttazzo, Nicolamaria Manes, and Fabrizio Giacomelli. Concise thoughts: Impact of output length on llm reasoning and cost. *arXiv preprint arXiv:2407.19825*, 2024.

Rylan Schaeffer, Joshua Kazdan, John Hughes, Jordan Juravsky, Sara Price, Aengus Lynch, Erik Jones, Robert Kirk, Azalia Mirhoseini, and Sanmi Koyejo. How do large language monkeys get their power (laws)? *arXiv preprint arXiv:2502.17578*, 2025.

John Schulman, Filip Wolski, Prafulla Dhariwal, Alec Radford, and Oleg Klimov. Proximal policy optimization algorithms. *arXiv preprint arXiv:1707.06347*, 2017.

Zhihong Shao, Peiyi Wang, Qihao Zhu, Runxin Xu, Junxiao Song, Xiao Bi, Haowei Zhang, Mingchuan Zhang, YK Li, Y Wu, et al. Deepseekmath: Pushing the limits of mathematical reasoning in open language models. *arXiv preprint arXiv:2402.03300*, 2024.

Guangming Sheng, Chi Zhang, Zilingfeng Ye, Xibin Wu, Wang Zhang, Ru Zhang, Yanghua Peng, Haibin Lin, and Chuan Wu. Hybridflow: A flexible and efficient rlhf framework. *arXiv preprint arXiv: 2409.19256*, 2024.

Taiwei Shi, Yiyang Wu, Linxin Song, Tianyi Zhou, and Jieyu Zhao. Efficient reinforcement finetuning via adaptive curriculum learning. *arXiv preprint arXiv:2504.05520*, 2025.

Petru Soviany, Radu Tudor Ionescu, Paolo Rota, and Nicu Sebe. Curriculum learning: A survey. *International Journal of Computer Vision*, 130(6):1526–1565, 2022.

Hanshi Sun, Momin Haider, Ruiqi Zhang, Huitao Yang, Jiahao Qiu, Ming Yin, Mengdi Wang, Peter Bartlett, and Andrea Zanette. Fast best-of-n decoding via speculative rejection. *arXiv preprint arXiv:2410.20290*, 2024.

Richard S Sutton, Andrew G Barto, et al. Reinforcement learning. *Journal of Cognitive Neuroscience*, 11(1):126–134, 1999.

Fahim Tajwar, Yiding Jiang, Abitha Thankaraj, Sumaita Sadia Rahman, J Zico Kolter, Jeff Schneider, and Ruslan Salakhutdinov. Training a generally curious agent. *arXiv preprint arXiv:2502.17543*, 2025.

Kimi Team, Angang Du, Bofei Gao, Bowei Xing, Changjiu Jiang, Cheng Chen, Cheng Li, Chenjun Xiao, Chenzhuang Du, Chonghua Liao, et al. Kimi k1. 5: Scaling reinforcement learning with llms. *arXiv preprint arXiv:2501.12599*, 2025.

Jason Wei, Xuezhi Wang, Dale Schuurmans, Maarten Bosma, Fei Xia, Ed Chi, Quoc V Le, Denny Zhou, et al. Chain-of-thought prompting elicits reasoning in large language models. *Advances in neural information processing systems*, 35:24824–24837, 2022.

Liang Wen, Yunke Cai, Fenrui Xiao, Xin He, Qi An, Zhenyu Duan, Yimin Du, Junchen Liu, Lifu Tang, Xiaowei Lv, et al. Light-r1: Curriculum sft, dpo and rl for long cot from scratch and beyond. *arXiv preprint arXiv:2503.10460*, 2025.

Tian Xie, Zitian Gao, Qingnan Ren, Haoming Luo, Yuqian Hong, Bryan Dai, Joey Zhou, Kai Qiu, Zhirong Wu, and Chong Luo. Logic-rl: Unleashing llm reasoning with rule-based reinforcement learning. *arXiv preprint arXiv:2502.14768*, 2025.

Yixuan Even Xu, Yash Savani, Fei Fang, and Zico Kolter. Not all rollouts are useful: Down-sampling rollouts in llm reinforcement learning. *arXiv preprint arXiv:2504.13818*, 2025.

An Yang, Beichen Zhang, Binyuan Hui, Bofei Gao, Bowen Yu, Chengpeng Li, Dayiheng Liu, Jianhong Tu, Jingren Zhou, Junyang Lin, et al. Qwen2. 5-math technical report: Toward mathematical expert model via self-improvement. *arXiv preprint arXiv:2409.12122*, 2024.

Yixin Ye, Zhen Huang, Yang Xiao, Ethan Chern, Shijie Xia, and Pengfei Liu. Limo: Less is more for reasoning. *arXiv preprint arXiv:2502.03387*, 2025.

Qiying Yu, Zheng Zhang, Ruofei Zhu, Yufeng Yuan, Xiaochen Zuo, Yu Yue, Tiantian Fan, Gaohong Liu, Lingjun Liu, Xin Liu, et al. Dapo: An open-source llm reinforcement learning system at scale. *arXiv preprint arXiv:2503.14476*, 2025.

A Omitted proof in Section 3

Proof 1 (Proof of Fact 1) *From the definition of $1-$smoothness, we know $-J_x(\theta)$ is 1-smooth if $J_x(\theta)$ is 1-smooth. We have*

$$-J_x(\theta+v) \le -J_x(\theta) + \nabla(-J_x(\theta))^\top v + \frac{1}{2}\|v\|^2$$

for any vector $v \in \mathbb{R}^d$ and parameter $\theta \in \mathbb{R}^d$. This implies

$$J_x(\theta+v) \;\ge\; J_x(\theta) + \nabla J_x(\theta)^\top v - \frac{1}{2}\|v\|^2.$$

Let $\widehat{g} := \widehat{\nabla_\theta J_x}(\theta)$ be an unbiased stochastic gradient so that $\mathbb{E}[\widehat{g}] = \nabla J_x(\theta)$. Applying this with $v = \widehat{g}$ and taking expectation,

$$\begin{aligned}
\mathbb{E}\big[J_x(\theta^+)\big] - J_x(\theta) &\ge \nabla J_x(\theta)^\top \mathbb{E}[\widehat{g}] - \frac{1}{2}\,\mathbb{E}\big[\|\widehat{g}\|^2\big] = \|\nabla J_x(\theta)\|^2 - \frac{1}{2}\Big(\mathbb{E}\|\widehat{g} - \mathbb{E}\widehat{g}\|^2 + \|\mathbb{E}\widehat{g}\|^2\Big) \\
&= \frac{1}{2}\,\|\nabla J_x(\theta)\|^2 - \frac{1}{2}\mathbb{E}\|\widehat{g} - \mathbb{E}\widehat{g}\|^2 \\
&= \frac{1}{2}\,\|\nabla J_x(\theta)\|^2 \left(1 - \frac{\mathbb{E}\|\widehat{g} - \mathbb{E}\widehat{g}\|^2}{\|\nabla J_x(\theta)\|^2}\right).
\end{aligned}$$

Invoking the definition of the Signal-to-Noise ratio in (9)*, we complete the proof.*

Now let's prove Theorem 3.1.

Proof 2 (Proof of Theorem 3.1) *Let π_θ be the LLM and fix a prompt $x \in \mathcal{X}$. For responses $y \in \mathcal{Y} \sim \pi_\theta(\cdot)$, we let $r(y)$ denote the binary reward which will be one if y is correct and zero otherwise. Let $\mathcal{C} \subset \mathcal{Y}$ be the set of correct responses, and $\mathcal{IC} \subset \mathcal{Y}$ be the set of incorrect responses.*

Define the pass rate of prompt x, evaluated by the model π_θ, as

$$\mathcal{P}_x(\theta) := \mathbb{P}_{y\sim\pi_\theta(\cdot|x)}\big(r(y)=1\big) = \sum_{y\in\mathcal{C}} \pi_\theta(y \mid x).$$

We define the SNR as in Equation (9)*, where $\widehat{\nabla_\theta J_x}(\theta)$ is defined as*

$$\widehat{\nabla_\theta J_x}(\theta) = \frac{1}{N}\sum_{i=1}^{N} \widehat{\mathcal{A}}(y_i)\cdot\nabla_\theta \log \pi_\theta(y_i \mid x), \quad \textit{where} \quad y_1, ..., y_N \overset{i.i.d.}{\sim} \pi_\theta(\cdot \mid x).$$

Here, $\widehat{\mathcal{A}}(y_i)$ is the advantage estimate for the response y_i. In RLOO, this is defined as

$$\widehat{\mathcal{A}}(y_i) := r(y_i) - \frac{1}{N-1}\sum_{j\neq i} r(y_j).$$

A simple fact is that the gradient estimate $\widehat{\nabla_\theta J_x}(\theta)$ is unbiased:

$$\begin{aligned}
\mathbb{E}\widehat{\nabla_\theta J_x}(\theta) &= \mathbb{E}\big[\widehat{\mathcal{A}}(y_1)\cdot\nabla_\theta \log\pi_\theta(y_1 \mid x)\big] \\
&= \mathbb{E}\big[r(y_1)\cdot\nabla_\theta \log\pi_\theta(y_1 \mid x)\big] - \frac{1}{N-1}\sum_{i\neq 1}\mathbb{E}\big[r(y_i)\cdot\nabla_\theta \log\pi_\theta(y_1 \mid x)\big] \\
&= \sum_{y_1\in\mathcal{C}} \pi_\theta(y_1 \mid x)\cdot\frac{\nabla_\theta\pi_\theta(y_1 \mid x)}{\pi_\theta(y_1 \mid x)} - \frac{1}{N-1}\sum_{i\neq 1}\mathbb{E}[r(y_i)]\cdot\underbrace{\mathbb{E}[\nabla_\theta\pi_\theta(y_1 \mid x)]}_{=0} \\
&= \nabla_\theta \mathcal{P}_x(\theta).
\end{aligned}$$

We define $R := (r(y_1), r(y_2), r(y_3), ..., r(y_N))^\top \in \{0,1\}^N$ as the random reward vector and $W := \sum_{i=1}^N r(y_i)$ as the empirical pass rate of the prompt x. Now let's consider the covariance matrix of $\widehat{\nabla_\theta J_x}(\theta)$. From the law of total variance, we know

$$\mathrm{Cov}\left[\widehat{\nabla_\theta J_x}(\theta)\right] = \mathrm{Cov}\left[\mathbb{E}\left[\widehat{\nabla_\theta J_x}(\theta)\middle| R(x)\right]\right] + \mathbb{E}\left[\mathrm{Cov}\left[\widehat{\nabla_\theta J_x}(\theta)\middle| R(x)\right]\right] \succeq \mathrm{Cov}\left[\mathbb{E}\left[\widehat{\nabla_\theta J_x}(\theta)\middle| R(x)\right]\right].$$

Here, $A \succeq B$ means $A - B$ is positive semi-definite (PSD) for two PSD matrices A and B. Now we calculate the conditional expectation. We have

$$\begin{aligned}
\mathbb{E}\left[\widehat{\nabla_\theta J_x}(\theta)\middle| R(x)\right] &= \frac{W}{N}\left(1-\frac{W-1}{N-1}\right)\cdot \mathbb{E}_{y\sim\pi_\theta(\cdot|x)}\left[\nabla_\theta \log \pi_\theta(y\mid x)\middle| r(y)=1\right] \\
&\quad + \frac{N-W}{N}\left(0-\frac{W}{N-1}\right)\cdot \mathbb{E}_{y\sim\pi_\theta(\cdot|x)}\left[\nabla_\theta \log \pi_\theta(y\mid x)\middle| r(y)=0\right] \\
&= \frac{W}{N}\left(1-\frac{W-1}{N-1}\right)\cdot \sum_{y\in\mathcal{C}} \frac{\pi_\theta(y\mid x)}{\mathcal{P}_x(\theta)}\cdot\frac{\nabla_\theta \pi_\theta(y\mid x)}{\pi_\theta(y\mid x)} \\
&\quad + \frac{N-W}{N}\left(0-\frac{W}{N-1}\right)\cdot \sum_{y\in\mathcal{IC}} \frac{\pi_\theta(y\mid x)}{1-\mathcal{P}_x(\theta)}\cdot\frac{\nabla_\theta \pi_\theta(y\mid x)}{\pi_\theta(y\mid x)} \\
&= \frac{W(N-W)}{N(N-1)}\cdot\frac{1}{\mathcal{P}_x(\theta)(1-\mathcal{P}_x(\theta))}\cdot\nabla_\theta\mathcal{P}_x(\theta).
\end{aligned}$$

Note that W follows a binomial distribution with parameters N and $\mathcal{P}_x(\theta)$. Recall the moments of binomial random variables, we have

$$\mathbb{E}\left[\mathbb{E}\left[\widehat{\nabla_\theta J_x}(\theta)\middle| R(x)\right]\right] = \mathbb{E}\widehat{\nabla_\theta J_x}(\theta) = \nabla_\theta\mathcal{P}_x(\theta)$$

and

$$\begin{aligned}
&\mathrm{Cov}\left(\mathbb{E}\left[\widehat{\nabla_\theta J_x}(\theta)\middle| R(x)\right]\right) \\
=\ & \frac{\mathbb{E}\big(W^2(N-W)^2\big)}{N^2(N-1)^2}\cdot\frac{1}{\mathcal{P}_x(\theta)^2(1-\mathcal{P}_x(\theta))^2}\cdot\nabla_\theta\mathcal{P}_x(\theta)\nabla_\theta\mathcal{P}_x(\theta)^\top - \nabla_\theta\mathcal{P}_x(\theta)\nabla_\theta\mathcal{P}_x(\theta)^\top \\
=\ & \left(\frac{1}{N}\cdot\frac{1}{\mathcal{P}_x(\theta)(1-\mathcal{P}_x(\theta))} + \frac{(N-2)(N-3)}{N(N-1)} - 1\right)\cdot\nabla_\theta\mathcal{P}_x(\theta)\nabla_\theta\mathcal{P}_x(\theta)^\top.
\end{aligned}$$

Therefore, we can upper bound the SNR via

$$\begin{aligned}
\textit{SNR} &= \frac{\|\mathbb{E}\widehat{\nabla_\theta J_x}(\theta)\|^2}{\mathrm{Tr}\left[\mathrm{Cov}\left[\widehat{\nabla_\theta J_x}(\theta)\right]\right]} \le \frac{\|\mathbb{E}\widehat{\nabla_\theta J_x}(\theta)\|^2}{\mathrm{Tr}\left[\mathrm{Cov}\left[\widehat{\nabla_\theta J_x}(\theta)\middle| R(x)\right]\right]} \\
&= \left[\frac{1}{N}\cdot\frac{1}{\mathcal{P}_x(\theta)(1-\mathcal{P}_x(\theta))} + \frac{(N-2)(N-3)}{N(N-1)} - 1\right]^{-1}.
\end{aligned}$$

Invoking the fact that $\mathcal{P}_x(\theta)(1-\mathcal{P}_x(\theta))$ is maximized when $\mathcal{P}_x(\theta) = 1/2$, we complete the proof.

B Theoretical justification of SPEED

Proof 3 (Proof of Theorem 4.1) *Fix N_{init} and N_{cont} with $N = N_{\mathsf{init}} + N_{\mathsf{cont}}$. Let $\overline{J}(\theta)$ denote the equivalent objective function of SPEED-RLOO and $\overline{J}_x(\theta)$ denote the objective function fo prompt x. We have $\overline{J}(\theta) = \mathbb{E}_{x\sim\mathcal{D}_\mathcal{X}}[\overline{J}_x(\theta)]$ by definition and analogously for their gradient. Now we are going to determine the concrete expression of $\nabla_\theta\overline{J}_x(\theta)$. From Algorithm 1, we have*

$$\nabla_\theta\overline{J}_x(\theta) = \mathbb{E}_{y_1,y_2,\ldots y_N}\left[\mathbb{I}\left(\sum_{i=1}^{N_{\mathsf{init}}} r(y_i)\notin\{0,N_{\mathsf{init}}\}\right)\cdot\frac{1}{N}\sum_{j=1}^{N}\widehat{\mathcal{A}}(y_j)\nabla\log\pi_\theta(y_j\mid x)\right], \tag{13}$$

where the expectation is over $y_1, y_2, ..., y_N \overset{i.i.d.}{\sim} \pi_\theta(\cdot\mid x)$, and $\widehat{\mathcal{A}}(y_j)$ is the advantage estimate for y_j given by

$$\widehat{\mathcal{A}}(y_j) = r(y_j) - \frac{1}{N-1}\sum_{k\neq j} r(y_k).$$

Denote the pass rate to x, evaluated by the model π_θ, as $\mathcal{P}_x(\theta)$. Now we decompose (13) *as*

$$\begin{aligned}\nabla_\theta \overline{J}_x(\theta) = &\underbrace{\mathbb{E}_{y_1,y_2,\dots y_N}\Big[\widehat{\mathcal{A}}(y_1)\nabla\log\pi_\theta(y_1\mid x)\Big]}_{I}\\ &\underbrace{-\mathbb{E}_{y_1,y_2,\dots y_N}\Big[\mathbb{I}\Big(\sum_{i=1}^{N_{\mathsf{init}}} r(y_i)=0\Big)\cdot\frac{1}{N}\sum_{j=1}^{N}\widehat{\mathcal{A}}(y_j)\nabla\log\pi_\theta(y_j\mid x)\Big]}_{II}\\ &\underbrace{-\mathbb{E}_{y_1,y_2,\dots y_N}\Big[\mathbb{I}\Big(\sum_{i=1}^{N_{\mathsf{init}}} r(y_i)=N_{\mathsf{init}}\Big)\cdot\frac{1}{N}\sum_{j=1}^{N}\widehat{\mathcal{A}}(y_j)\nabla\log\pi_\theta(y_j\mid x)\Big]}_{III}.\end{aligned}$$

From the independence among all responses, one has

$$\begin{aligned}I &= \mathbb{E}_{y_1,y_2,\dots y_N}\Big[r(y_1)\nabla_\theta\log\pi_\theta(y_1\mid x)\Big]-\frac{1}{N-1}\sum_{k\neq 1}\mathbb{E}_{y_1,y_2,\dots y_N}\Big[r(y_k)\nabla_\theta\log\pi_\theta(y_1\mid x)\Big]\\ &= \nabla_\theta\mathcal{P}_x(\theta)-\frac{1}{N-1}\sum_{k\neq 1}\mathbb{E}_{y_1,y_2,\dots y_N}\big[r(y_k)\big]\cdot\underbrace{\mathbb{E}_{y_1,y_2,\dots y_N}\big[\nabla_\theta\log\pi_\theta(y_1\mid x)\big]}_{=0}\\ &= \nabla_\theta\mathcal{P}_x(\theta).\end{aligned}$$

The expectand in II vanishes if $\sum_{i=1}^{N_{\mathsf{init}}} r(y_i)\neq 0$. Analogously, the expectand in III vanished if $\sum_{i=1}^{N_{\mathsf{init}}} r(y_i)\neq N_{\mathsf{init}}$. Let's denote

$$\mathcal{E}_0 := \Big\{\sum_{i=1}^{N_{\mathsf{init}}} r(y_i)=0\Big\},\quad \mathcal{E}_1 := \Big\{\sum_{i=1}^{N_{\mathsf{init}}} r(y_i)=N_{\mathsf{init}}\Big\}.$$

We have

$$\begin{aligned}&\mathbb{E}\big[\nabla_\theta\log\pi_\theta(y_1\mid x)\big|\mathcal{E}_0\big]=-\frac{\nabla_\theta\mathcal{P}_x(\theta)}{1-\mathcal{P}_x(\theta)},\quad \mathbb{E}\big[\nabla_\theta\log\pi_\theta(y_1\mid x)\big|\mathcal{E}_1\big]=\frac{\nabla_\theta\mathcal{P}_x(\theta)}{\mathcal{P}_x(\theta)},\\ &\mathbb{E}\big[\nabla_\theta\log\pi_\theta(y_N\mid x)\big|\mathcal{E}_0\big]=0,\quad \mathbb{E}\big[\nabla_\theta\log\pi_\theta(y_N\mid x)\big|\mathcal{E}_1\big]=0,\\ &\mathbb{E}\big[r(y_N)\nabla_\theta\log\pi_\theta(y_N\mid x)\big|\mathcal{E}_0\big]=\nabla_\theta\mathcal{P}_x(\theta),\quad \mathbb{E}\big[r(y_N)\nabla_\theta\log\pi_\theta(y_N\mid x)\big|\mathcal{E}_1\big]=\nabla_\theta\mathcal{P}_x(\theta).\end{aligned}\tag{14}$$

Therefore, one has

$$\begin{aligned}&\mathbb{E}_{y_1,y_2,\dots y_N}\Big[\mathbb{I}\Big(\sum_{i=1}^{N_{\mathsf{init}}} r(y_i)=0\Big)\cdot\frac{1}{N}\sum_{j=1}^{N}\widehat{\mathcal{A}}(y_j)\nabla\log\pi_\theta(y_j\mid x)\Big|\mathcal{E}_0\Big]\\ =\;&\mathbb{E}_{y_1,y_2,\dots y_N}\Big[\frac{1}{N}\sum_{j=1}^{N} r(y_j)\Big(\nabla_\theta\log\pi_\theta(y_j\mid x)-\frac{1}{N-1}\sum_{k\neq j}\nabla_\theta\log\pi_\theta(y_k\mid x)\Big)\Big|\mathcal{E}_0\Big]\\ =\;&\mathbb{E}\Big[\frac{1}{N}\sum_{j=N_{\mathsf{init}}+1}^{N} r(y_j)\nabla_\theta\log\pi_\theta(y_j\mid x)\Big|\mathcal{E}_0\Big]-\mathbb{E}\Big[\frac{1}{N(N-1)}\sum_{j=N_{\mathsf{init}}+1}^{N} r(y_j)\sum_{k\neq j}\nabla_\theta\log\pi_\theta(y_k\mid x)\Big)\Big|\mathcal{E}_0\Big]\\ =\;&\frac{N_{\mathsf{cont}}}{N}\nabla_\theta\mathcal{P}_x(\theta)-\frac{N_{\mathsf{cont}}}{N(N-1)}\mathbb{E}\big[r(y_N)\big|\mathcal{E}_0\big]\cdot\mathbb{E}\big[\sum_{k\neq N}\nabla_\theta\log\pi_\theta(y_k\mid x)\big|\mathcal{E}_0\big]\\ =\;&\frac{N_{\mathsf{cont}}}{N}\nabla_\theta\mathcal{P}_x(\theta)+\frac{N_{\mathsf{cont}}N_{\mathsf{init}}}{N(N-1)}\frac{\mathcal{P}_x(\theta)}{1-\mathcal{P}_x(\theta)}\cdot\nabla_\theta\mathcal{P}_x(\theta).\end{aligned}$$

Therefore, we have

$$II=\big(1-\mathcal{P}_x(\theta)\big)^{N_{\mathsf{init}}}\Big(\frac{N_{\mathsf{cont}}}{N}+\frac{N_{\mathsf{cont}}N_{\mathsf{init}}}{N(N-1)}\cdot\frac{\mathcal{P}_x(\theta)}{1-\mathcal{P}_x(\theta)}\Big)\cdot\nabla_\theta\mathcal{P}_x(\theta).$$

Analogously, we have

$$
\begin{aligned}
&\mathbb{E}_{y_1,y_2,\dots y_N}\left[\mathbb{I}\Big(\sum_{i=1}^{N_{\mathsf{init}}} r(y_i)=N_{\mathsf{init}}\Big)\cdot\frac{1}{N}\sum_{j=1}^{N}\widehat{\mathcal{A}}(y_j)\nabla\log\pi_\theta(y_j\mid x)\Big|\mathcal{E}_1\right]\\
=\;&\mathbb{E}_{y_1,y_2,\dots y_N}\left[\frac{1}{N}\sum_{j=1}^{N} r(y_j)\Big(\nabla_\theta\log\pi_\theta(y_j\mid x)-\frac{1}{N-1}\sum_{k\neq j}\nabla_\theta\log\pi_\theta(y_k\mid x)\Big)\Big|\mathcal{E}_1\right]\\
=\;&\frac{N_{\mathsf{init}}}{N}\mathbb{E}\big[\nabla_\theta\log\pi_\theta(y_1\mid x)\big|\mathcal{E}_1\big]-\frac{N_{\mathsf{init}}}{N(N-1)}\sum_{k\neq 1}\mathbb{E}\big[\nabla_\theta\log\pi_\theta(y_k\mid x)\big|\mathcal{E}_1\big]\\
&\qquad+\frac{N_{\mathsf{cont}}}{N}\mathbb{E}\big[r(y_N)\nabla_\theta\log\pi_\theta(y_N\mid x)\big|\mathcal{E}_1\big]-\frac{N_{\mathsf{cont}}}{N(N-1)}\sum_{k\neq N}\mathbb{E}\big[r(y_N)\nabla_\theta\log\pi_\theta(y_k\mid x)\big|\mathcal{E}_1\big]\\
=\;&\left(\frac{N_{\mathsf{init}}}{N}-\frac{N_{\mathsf{init}}(N_{\mathsf{init}}-1)}{N(N-1)}\right)\cdot\frac{\nabla\mathcal{P}_x(\theta)}{\mathcal{P}_x(\theta)}\\
&\qquad+\frac{N_{\mathsf{cont}}}{N}\nabla_\theta\mathcal{P}_x(\theta)-\frac{N_{\mathsf{cont}}}{N(N-1)}\mathcal{P}_x(\theta)\cdot\sum_{k\neq N}\mathbb{E}\big[\nabla_\theta\log\pi_\theta(y_N\mid x)\big|\mathcal{E}_1\big]\\
=\;&\frac{N_{\mathsf{init}}N_{\mathsf{cont}}}{N(N-1)}\cdot\frac{\nabla_\theta\mathcal{P}_x(\theta)}{\mathcal{P}_x(\theta)}+\frac{N_{\mathsf{cont}}}{N}\nabla_\theta\mathcal{P}_x(\theta)-\frac{N_{\mathsf{init}}N_{\mathsf{cont}}}{N(N-1)}\cdot\nabla_\theta\mathcal{P}_x(\theta)\\
=\;&\frac{N_{\mathsf{cont}}}{N}\nabla_\theta\mathcal{P}_x(\theta)+\frac{N_{\mathsf{init}}N_{\mathsf{cont}}}{N(N-1)}\cdot\frac{1-\mathcal{P}_x(\theta)}{\mathcal{P}_x(\theta)}\cdot\nabla_\theta\mathcal{P}_x(\theta).
\end{aligned}
$$

Therefore, one has

$$
\textit{III}=\mathcal{P}_x(\theta)^{N_{\mathsf{init}}}\left(\frac{N_{\mathsf{cont}}}{N}+\frac{N_{\mathsf{init}}N_{\mathsf{cont}}}{N(N-1)}\frac{1-\mathcal{P}_x(\theta)}{\mathcal{P}_x(\theta)}\right)\cdot\nabla_\theta\mathcal{P}_x(\theta).
$$

This indicates

$$
\begin{aligned}
\nabla_\theta\overline{J}_x(\theta)=\Bigg[&1-\frac{N_{\mathsf{cont}}}{N}\Big(\mathcal{P}_x(\theta)^{N_{\mathsf{init}}}+\big(1-\mathcal{P}_x(\theta)\big)^{N_{\mathsf{init}}}\Big)\\
&-\frac{N_{\mathsf{init}}N_{\mathsf{cont}}}{N(N-1)}\Big(\mathcal{P}_x(\theta)\big(1-\mathcal{P}_x(\theta)\big)^{N_{\mathsf{init}}-1}+\big(1-\mathcal{P}_x(\theta)\big)\mathcal{P}_x(\theta)^{N_{\mathsf{init}}-1}\Big)\Bigg]\nabla_\theta\mathcal{P}_x(\theta).
\end{aligned}
$$

Integrating the gradient gives:

$$
\overline{J}_x(\theta)=\Phi(\mathcal{P}_x(\theta)),
$$

where

$$
\begin{aligned}
\Phi(p)=\;&p-\frac{N_{\mathsf{cont}}}{N(N_{\mathsf{init}}+1)}\Big(p^{N_{\mathsf{init}}+1}-(1-p)^{N_{\mathsf{init}}+1}\Big)\\
&+\frac{N_{\mathsf{cont}}}{N(N-1)(N_{\mathsf{init}}+1)}\Big(\big(1+N_{\mathsf{init}}p\big)\big(1-p\big)^{N_{\mathsf{init}}}-p^{N_{\mathsf{init}}}\big(N_{\mathsf{init}}\big(1-p\big)+1\big)\Big)+\textit{Const.}
\end{aligned}
$$

Moreover, since

$$
\begin{aligned}
\Phi'(p)&=1-\frac{N_{\mathsf{cont}}}{N}\big(p^{N_{\mathsf{init}}}+(1-p)^{N_{\mathsf{init}}}\big)-\frac{N_{\mathsf{init}}N_{\mathsf{cont}}}{N(N-1)}\big(p(1-p)^{N_{\mathsf{init}}-1}+(1-p)p^{N_{\mathsf{init}}-1}\big)\\
&\geq 1-\frac{N_{\mathsf{cont}}}{N}-\frac{N_{\mathsf{init}}N_{\mathsf{cont}}}{N(N-1)}\\
&\geq 1-\frac{N_{\mathsf{cont}}}{N}-\frac{N_{\mathsf{init}}}{N}=0. \qquad (N_{\mathsf{cont}}\leq N-1)
\end{aligned}
$$

Therefore, $\Phi(\cdot)$ is monotonically increasing and hence, for every prompt $x\in\mathcal{X}$, one has

$$
\mathbb{E}_{y\sim\pi_\theta(\cdot|x)}[r(y)]=1 \quad \textit{maximizes} \quad \Phi(\mathbb{E}_{y\sim\pi_\theta(\cdot|x)}[r(y)]).
$$

This completes the proof.

C Full Algorithm

Now we describe our full algorithm combined with the data buffer and the pre-fetching mechanism.

Algorithm 2 SELECTIVE PROMPTING WITH EFFICIENT ESTIMATION OF DIFFICULTY (**SPEED**)

Input: An auto-regressive generative model π_θ, a binary reward model r, difficulty filter thresholds $P_{\text{low}}, P_{\text{high}}$, the number of generations in both phases $N_{\text{init}}, N_{\text{cont}}$, total number of (training) steps T, training batch size B.

Initialize the data buffer $\mathcal{D}_{\text{buffer}} = \emptyset$. Initialize the number of training steps $t = 0$.
Initialize the data cache $\mathcal{D}_{\text{accepted}} = \emptyset$.
while $t < T$ **do**
  if $|\mathcal{D}_{\text{buffer}}| < B$ **then** # We are not ready for training.
    Fetch a batch of prompt $\mathcal{D}_{\text{new}}$ from the data loader.
    if $\mathcal{D}_{\text{accepted}} \neq \emptyset$ **then**
      Batch the prompts: $\mathcal{D}_{\text{infer}} \leftarrow \mathcal{D}_{\text{accepted}} \cup \mathcal{D}_{\text{new}}$. # Batch the prompts.
    end if
    Call the inference engine on $\mathcal{D}_{\text{infer}}$ to generate N_{init} responses for prompts in $\mathcal{D}_{\text{new}}$, and N_{cont} responses for prompts in $\mathcal{D}_{\text{accepted}}$.
    $\mathcal{D}_{\text{buffer}} \leftarrow \mathcal{D}_{\text{buffer}} \cup \mathcal{D}_{\text{accepted}}$. # Add completed prompts to the buffer for training.
    for $x \in \mathcal{D}_{\text{new}}$ **do** # Compute the pass rate for new prompts
      $\text{PASSRATE}(x) \leftarrow \frac{1}{N_{\text{init}}} \sum_{i=1}^{N_{\text{init}}} \mathbb{I}(\text{response}_i \text{ is correct})$
    end for
    $\mathcal{D}_{\text{accepted}} \leftarrow \mathcal{D}_{\text{accepted}} \cup \{x \in \mathcal{D}_{\text{new}} : P_{\text{low}} < \text{PASSRATE}(x) < P_{\text{high}}\}$. Update the set of qualified prompts.
  else
    Sample $\mathcal{D}_{\text{train}} \sim \mathcal{D}_{\text{buffer}}$ with $|\mathcal{D}_{\text{train}}| = B$. # Get one batch of data for training.
    Train one RL step on $\mathcal{D}_{\text{train}}$.
    $\mathcal{D}_{\text{buffer}} \leftarrow \mathcal{D}_{\text{buffer}} - \mathcal{D}_{\text{train}}$. # Update the data buffer.
    $t \leftarrow t + 1$. # Record the training step
  end if
end while

Output: The trained model π_θ.

D Figures of More Experimental Results

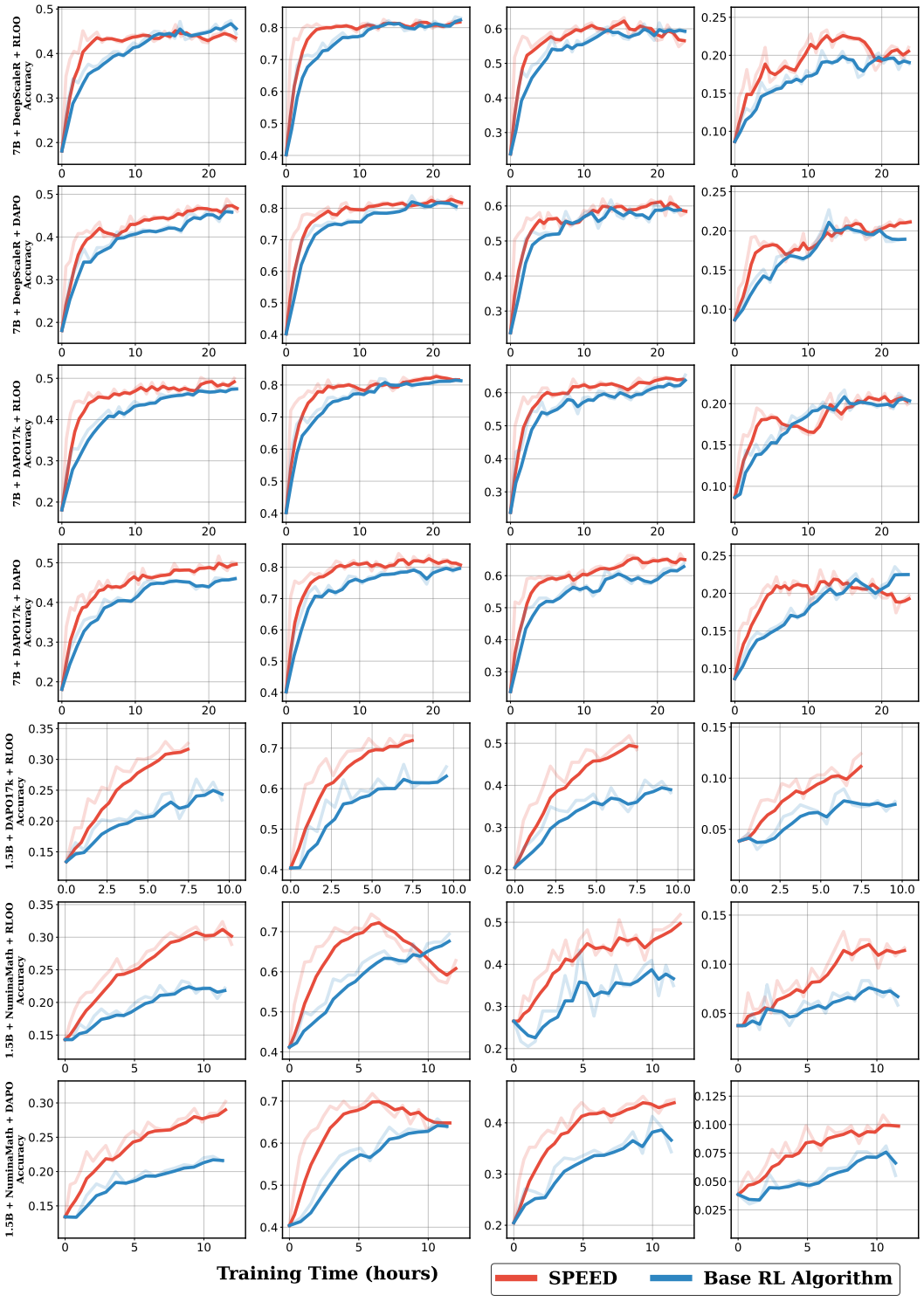

Figure 6: Validation accuracy on various mathematical reasoning benchmarks for SPEED-variants of RL algorithms, and base RL algorithms. The initial model used is Qwen2.5-Math-7B (for the top 4 rows) and Qwen2.5-Math-1.5B (for the bottom 3 rows). Y-axis labels follow the pattern 'Model size + Training set + Base RL algorithm'. We use three training dataset: NuminaMath [Li et al., 2024], DAPO-17k (without 1k held-out validation set) [Yu et al., 2025], and DeepScaleR [Luo et al., 2025], and we use 2 base RL algorithms: RLOO [Ahmadian et al., 2024] and DAPO [Yu et al., 2025]. The lighter curves represent raw accuracy results, while the bold curves indicate smoothed results obtained via an exponential moving average.